11-1-2007

Macroscopic Consequences of Calcium Signaling in Microdomains: A First-Passage-Time Approach

Robert Rovetti

Loyola Marymount University

Citation / Publisher Attribution

Rovetti, Robert [et al]. (2007) "Macroscopic Consequences of Calcium Signaling in Microdomains: A First-Passage-Time Approach." *Physical Review E 76*, 051920.

Macroscopic consequences of calcium signaling in microdomains: A first-passage-time approach

Robert Rovetti,[1] Kunal K. Das,[2] Alan Garfinkel,[3] and Yohannes Shiferaw[4]
[1]*Department of Biomathematics, University of California, Los Angeles, California 90095, USA*
[2]*Department of Physics, Fordham University, Bronx, New York 10458, USA*
[3]*Department of Medicine, University of California, Los Angeles, California 90095, USA*
[4]*Department of Physics and Astronomy, California State University, Northridge, California 91330, USA*
(Received 25 January 2007; published 29 November 2007)

Calcium (Ca) plays an important role in regulating various cellular processes. In a variety of cell types, Ca signaling occurs within microdomains where channels deliver localized pulses of Ca activating a nearby collection of Ca-sensitive receptors. The small number of channels involved ensures that the signaling process is stochastic. The aggregate response of several thousand of these microdomains yields a whole-cell response which dictates the cell behavior. Here, we study the statistical properties of a population of these microdomains in response to a trigger signal. We use a first-passage-time approach to show analytically how Ca release in the whole cell depends on properties of Ca channels within microdomains. Using these results we explain for the first time the underlying mechanism for the graded relationship between Ca influx and Ca release in cardiac cells.

DOI: 10.1103/PhysRevE.76.051920 PACS number(s): 87.16.Xa, 87.16.Uv

INTRODUCTION

The use of Ca-sensitive receptors is ubiquitous in the design of signal transduction processes [1]. A basic feature of this design is the distribution of localized regions near the cell surface called Ca microdomains [2], where Ca-permeable channels on the cell membrane are positioned adjacent to Ca-sensitive receptors within the cell. Signaling occurs when a channel on the membrane delivers a small amount of extracellular Ca into the microdomain; the subsequent rise of the local Ca concentration "triggers" the nearby receptor channels to release large amounts of Ca from enclosed Ca stores within the cell. In this way, a trigger input can induce a large response signal, stimulating downstream cellular processes. This architecture is utilized in cardiac cells where voltage-sensitive L-type Ca channels (LCC) on the cell membrane trigger the opening of a cluster of Ca-sensitive ryanodine receptor (RyR) channels [3] signaling cell contraction. A similar architecture is found at synaptic endings in neurons, where localized pulses of Ca signal transmitter release [2].

Experimental studies in cardiac cells have shown that the total amount of Ca released into the cell is smoothly graded with respect to the total Ca entering the cell via LCCs [3,4]. This response, termed "graded release," is a central feature of the coupling between membrane voltage and intracellular Ca [3]. Although it is well established that variable local activation of microdomains allows for a variable release [5], to date it is not understood how the stochastic signaling between LCCs and RyR clusters relates to macroscopic graded release. Computer simulation studies [6–10] of large numbers of stochastic microdomains can replicate graded release. However, these numerical studies do not shed light on the mechanisms which underly graded release. Additionally, the dynamics of RyR-like Ca-sensitive channel clusters have been examined [11–13], but only in the context of spontaneous self-activation without an independent trigger. In this paper we analyze the stochastic interaction between triggering LCCs and Ca-sensistive RyR clusters. We treat the aggregate of microdomains in a cell as a stochastic ensemble, and derive an accurate analytical expression relating the influx of Ca to the total amount of intracellular Ca released due to the dynamics of Ca channel clusters. Our analytical results reproduce the experimental features of graded release, and explicitly show how trigger-response relationships, critical to cell function, are related to the stochastic interaction of ion channels.

PHYSICAL MODEL

The basic architecture of Ca signaling in cardiac cells is shown schematically in Fig. 1(a). Here, the signaling occurs within microdomains where a few (1–5) voltage-sensitive LCCs on the cell membrane are in close proximity to a cluster of 50–200 Ca-sensitive RyRs [3]. The RyRs gate the flow of Ca from the sarcoplasmic reticulum (SR), an internal Ca store with a concentration roughly 10^4 times greater than in the cytosol (the volume of the cell outside of the SR). Each microdomain is roughly shaped like a pill box of height $\sim$10 nm and diameter $\sim$100 nm; a typical cardiac cell has $\sim 10^4$ microdomains distributed throughout the cell.

To model ion channels within the microdomain we use a Markov state approach as illustrated in Fig. 1(b). The single channel properties of LCCs have been studied extensively [14]; here we model a single LCC using two closed states which can transition to a Ca-permeable open state [24]. The membrane voltage (V) dependence of LCCs appears in the transition rates between closed states $[\alpha_1(V), \beta_1(V)]$, while transition rates to and from the open state (α and β) are voltage independent.

The basic properties of the activation kinetics of RyRs are known [15], and it is believed that the open probability is regulated by several Ca binding sites acting cooperatively on the receptor. Here, we employ a minimal model that incorporates these essential features, using an opening rate k_+c^2 with a nonlinear Ca dependence (c denotes the local micro-

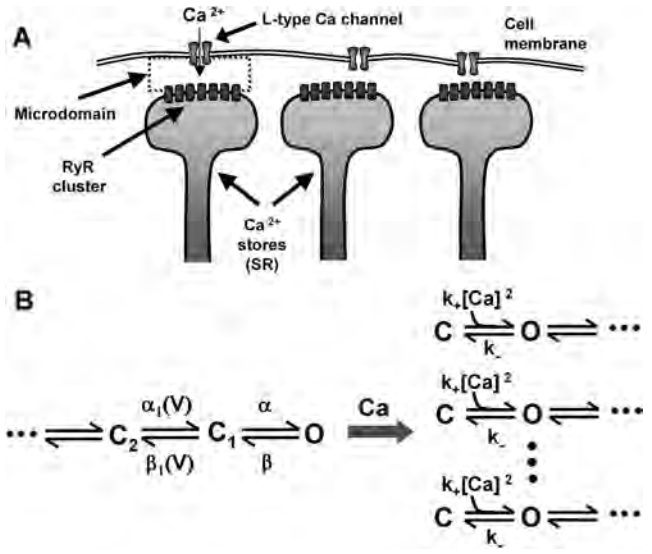

FIG. 1. (a) Illustration of Ca-mediated signaling between LCC and RyR channels in cardiac cells. Ca is injected into the cell via the LCCs and triggers the opening of RyR channels in the immediate vicinity. (b) Markov state models for LCC (left) and RyRs (right). The vertical dots indicate many (~50–200) RyRs; horizontal dots represent possible deeper states.

domain Ca concentration) and a constant closing rate k_-. A model with similar activation kinetics is used in a previous numerical study by Stern *et al.* [9]. Since the interaction between LCCs and RyRs is dominated by the activation kinetics, we have neglected the deeper states in the Markov scheme which describe slower inactivation and recovery processes.

When a cardiac cell is stimulated, the rise of the membrane voltage leads to a dramatic increase in the open probability of LCCs. The subsequent Ca entry into the cell induces Ca release via RyR channels. High resolution optical imaging of Ca [16] in cardiac cells confirms local elevations in Ca, referred to as Ca "sparks" which correspond to the triggered release of Ca from the SR. In our model, a Ca spark is activated when an LCC opening leads to a rise in microdomain Ca and an initial opening of a few RyR channels, which is sufficient to induce further openings of the RyRs in the cluster. This process is autocatalytic owing to the large Ca concentration gradient across the RyR channels. We say that a spark has occurred when a substantial fraction of the RyR channels in the cluster have opened. However, it is important to note that from the experimental standpoint, it is not known exactly how many RyR channels need to open to induce this autocatalytic process. In this study we assume that roughly 10 of the 50–200 RyR channels need to open in order to induce a Ca spark. A more general treatment, where this restriction is relaxed, will be addressed in a forthcoming publication.

The collective effect of these individual sparks is a rise in global cell Ca. Although local Ca spark amplitudes may vary among microdomain sites, they are known to be relatively constant at a given site due to local geometry of the microdomain and the size of the RyR cluster [16]. For a large number of microdomains, the interdependence of Ca release and the whole cell current is dictated by the number of release events recruited [5,17].

THEORETICAL MODEL

Here we consider the sequence of local events by which a quiescent microdomain is induced to spark in response to an LCC opening, and relate those events to the whole-cell response. If we denote ΔN_S to be the total number of new sparks recruited in the cell during a small time interval Δt, then

$$\Delta N_S = N_d P_{C_1} \alpha \Delta t P_S(i_{Ca}), \tag{1}$$

where N_d is the number of microdomains in the cell; $P_{C_1}\alpha\Delta t$ is the probability that an LCC initially found in the final closed state C_1 (with probability P_{C_1}) will transition to the open state O (at rate α) in time interval Δt; and $P_S(i_{Ca})$ denotes the probability that the LCC opening will trigger a spark in response to the influx of a Ca current of magnitude i_{Ca}. The key quantity relating local channel interactions to the whole-cell response is then the rate of spark recruitment $R_S = \Delta N_S / \Delta t$, which depends on the trigger-response interaction described by P_S.

To compute P_S we first note that Ca ions inside the cell diffuse in the range ~50–300 $\mu m^2/s$ [18], and thus equilibrate over the length scale (~0.1 μm) of the microdomain much faster (~0.01 ms) than the typical channel transition times (~1 ms). Fast diffusion yields

$$c \approx c_o + (\tau/v)(n i_{RyR} + k i_{Ca}), \tag{2}$$

where c_o is the resting Ca concentration outside of the microdomain of volume v; τ is the time constant of diffusion out of the microdomain; n and k are the number of open RyR and LCC channels, respectively; and i_{RyR} and i_{Ca} are the fluxes, in ions per unit time, through the respective single open channels. We set $i_{RyR} = g c_{sr}$, valid for small c, where g is the conductance of a single RyR channel and c_{sr} is the Ca concentration in the SR. Both the current i_{Ca} through an open LCC as well as the channel kinetics are dependent on membrane voltage; the LCC open time t' has the exponential distribution

$$f_O(t') = \beta \exp(-\beta t'). \tag{3}$$

Since there are only a few LCCs in the microdomain, each with small open probability [14], we simplify the system further by assuming only one LCC in each microdomain, so that $k = 0$ or 1.

To describe the state n of the RyR cluster we implement a master equation approach [12,19] for the probability $P(n,t)$ that n out of N total RyR channels in the cluster are open. This is given by

$$\frac{dP(n,t)}{dt} = r_+(n-1)P(n-1,t) + r_-(n+1)P(n+1,t) - [r_+(n) + r_-(n)]P(n,t), \tag{4}$$

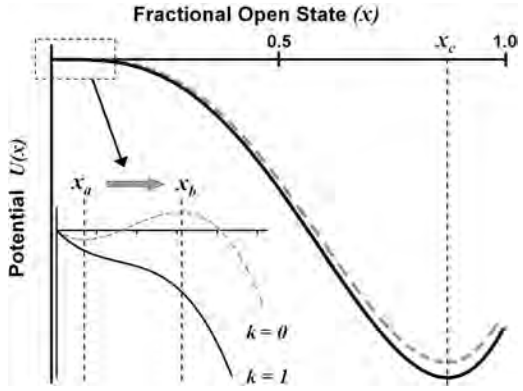

FIG. 2. Effective potential landscape $U(x)$ corresponding to closed ($k=0$; dashed line) or open ($k=1$; solid line) LCC. Inset: Barrier near origin disappears when i_{Ca} is large enough. Parameters here are $i_{Ca}=0.06$ pA, $g=0.520$ $\mu m^3 s^{-1}$ and $c_o=5$ μM.

with the forward transition rate $r_+(n)=k_+c^2(N-n)$ and backward transition rate $r_-(n)=k_-n$. Note that the Ca concentration c regulating the forward rate is itself a function of n, the number of open RyR channels [see Eq. (2)]. Thus $r_+(n)$ is a third-degree polynomial in the number of open channels n, and a spark occurs when n rapidly approaches N.

ANALYTICAL SOLUTION BASED ON FIRST PASSAGE TIME

We seek a solution that describes the response of the RyR cluster, governed by Eq. (4), to a stochastic trigger signal, governed by Eq. (3). For large N, we can use well-known approximation methods [20] to reduce the one-step (birth-death) process to its corresponding Fokker-Planck equation (FPE), which we can write, in terms of the fraction $x=n/N$ of open channels, as

$$\frac{\partial p(x,t)}{\partial t} = -\frac{\partial}{\partial x}[f(x)p(x,t)] + \frac{1}{2N}\frac{\partial^2}{\partial x^2}[h(x)p(x,t)], \quad (5)$$

with drift coefficient $f(x)=[r_+(Nx)-r_-(Nx)]/N$ and diffusion coefficient $h(x)/N=[r_+(Nx)+r_-(Nx)]/N^2$. The diffusion term scales as $1/N$ implying the increasingly deterministic nature with larger cluster size [21].

The equivalent Langevin description corresponding to this FPE implies time evolution of the *mean* open fraction $\langle x\rangle$ dictated by the equation $\frac{d\langle x\rangle}{dt}=f(\langle x\rangle)$. Therefore $f(x)=0$ determines the stationary points of x. The deterministic component of the dynamics can be conveniently visualized in terms of a potential $U(x)=-\int_0^x f(x')dx'$ as shown in Fig. 2. The dynamics of spark activation occurs when x is small; in this regime $f(x)$ is well approximated by a quadratic $f(x)\approx\sigma+\mu x+k_+q^2x^2$ where, using Eq. (2), $\sigma=k_+s^2$ and $\mu=-k_-+2k_+qs$, and where $q=N(\tau/v)gc_{sr}$ and $s=c_o+(\tau/v)ki_{Ca}$.

In order to compute the probability of sparking it is necessary to evaluate the effect of an LCC opening on the potential landscape, whose form follows two scenarios:

Scenario I: $k=0$ (the upper trace in Fig. 2) which corresponds to the LCC being *closed* in a microdomain, so that the parameter $s=c_0$ (a small background concentration), and therefore $\mu<0$ and the quadratic equation $f(x)=0$ has two positive solutions. There is a stable solution $x_a\approx(k_+/k_-)c_o^2$ close to zero, corresponding to an inactive cluster with very few channels open. More importantly there is an unstable point at position $x_b\approx(k_-/k_+)q^{-2}$ which acts as a *potential barrier* separating the closed and open cluster states. In this study we assume that the number of open RyR channels required to reach threshold is roughly $Nx_b\approx10$. We note that in the limit when $Nx_b\approx1$, then only one channel needs to open for the whole cluster to fire; we do not consider this limit here since the reduction of the master equation to the Fokker-Planck equation would not be valid in that limit.

Scenario II: $k=1$ (the lower trace in Fig. 2) which corresponds to the LCC being *open* in a microdomain, so that s is now larger. For moderate values of s the potential barrier is lowered, while for higher values (so that $\mu>0$) the potential barrier may vanish completely.

In either scenario, the cubic term neglected in the quadratic approximation for $f(x)$ can yield a second stable point x_c far from the origin denoting a nearly fully open cluster. At that point the cluster state is beyond the potential barrier, so x_c has no role in the spark activation transition dynamics and is not considered further.

From these two scenarios it is possible to compute how often an LCC opening will induce a spark. At first, when the LCC is closed, the RyR cluster will be in the "inactive" state close to x_a, and the potential barrier is high. However, when the LCC opens the barrier height is substantially reduced and the system can escape from the vicinity of x_a. Thus, we argue that: (i) If the LCC remains open until *after* x crosses x_b, then it is almost certain that a spark will occur as x proceeds to x_c; (ii) but if the channel closes *before* x crosses x_b, then a spark is *not* likely since as the barrier returns the cluster state is inclined to return to x_a. Thus, given a passage time t from x_a to x_b, the LCC open time t', obeying the exponential distribution $f_O(t')$, must exceed t. The sparking probability is then given by

$$P_S(i_{Ca}) = \int_0^\infty dt\, e^{-\beta t} P(x_a, x_b, i_{Ca}; t), \quad (6)$$

where $P(x_a, x_b, i_{Ca}; t)$ is the first-passage-time density (FPTD) from x_a to x_b for the system given by Eq. (5).

Equation (6) is also the Laplace transform (LT) of the FPTD, which can be expressed in terms of the solutions of the LT transform of the *adjoint* of the original FPE [Eq. (5)], as shown in a classic paper by Darling and Siegert [22]. Linearizing the drift and diffusion coefficients so that $f(x)=\sigma+\mu x$ and $h(x)=\sigma+\gamma x$, where $\gamma=k_-+2k_+qs$, the LT of the adjoint FPE can be written as a confluent hypergeometric differential equation, which has the linearly independent solutions $u_1(x)=M[m_1,m_2,y(x)]$ and $u_2(x)=y(x)^{1-m_2}M[1+m_1-m_2,2-m_2,y(x)]$, where M denotes Kummer's function [23] with arguments $m_1=-\beta/\mu$, $m_2=2N\sigma(\gamma-\mu)/\gamma^2$ and $y(x)=-2N\mu(\sigma+\gamma x)/\gamma^2$. Imposing a *reflecting* boundary condition at $x=0$, since the master equation [Eq. (4)] does not admit negative valued states, the probability of sparking can be written [22] as

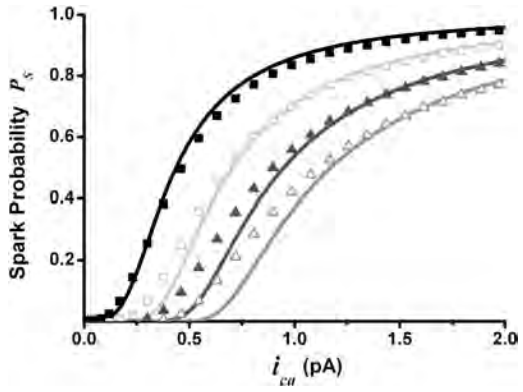

FIG. 3. Analytical (curves) and numerically simulated (symbols) sparking probability P_S as a function of i_{Ca}, conditional upon an LCC activation, for conductances $g=0.910$ (■), 0.628 (□), 0.491 (▲), and 0.416 (△) $\mu m^3\,s^{-1}$.

$$P_S(i_{Ca}) = \frac{u_1(x_a)/u_1'(0) - u_2(x_a)/u_2'(0)}{u_1(x_b)/u_1'(0) - u_2(x_b)/u_2'(0)}, \tag{7}$$

where $u_1'(0)$ and $u_2'(0)$ are the derivatives of the independent solutions evaluated at the origin. Equation (7) gives a full description of the sparking probability given a trigger current i_{Ca} with duration obeying the distribution f_O.

Limiting Cases: The analytic formula for the spark probability [Eq. (7)] can be simplified further in the limit of large or small LCC current (i_{Ca}). Using the asymptotic form of Kummer's function [23], for large i_{Ca} we have

$$P_S \sim \left(\frac{\sigma + \gamma x_a}{\sigma + \gamma x_b}\right)^{\beta/\mu}. \tag{8}$$

In this limit, in which the triggering Ca current is strong, the response is governed by the mean open time of the LCC, and does not strongly depend on the stochastic properties of the RyR cluster. For small i_{Ca} an activation barrier must be surmounted, and stochastic fluctuations due to the N RyR channels dictate the probability for sparking in response to the weaker Ca current. In this regime, to leading order we have

$$P_S \sim \exp\left(\frac{2\mu}{\gamma} N(x_b - x_a)\right), \tag{9}$$

showing the strong dependence on RyR cluster size N.

COMPARISON TO NUMERICS AND EXPERIMENTAL DATA

Comparison to numerical solution: In order to check the validity of this analytical result we simulate independent Monte Carlo trajectories of the master equation to estimate the probability of sparking (P_S) given an LCC opening at time $t=0$, in an ensemble of 100,000 microdomains whose clusters are initially closed ($n \approx N x_a$). Within each unit a single LCC is opened for a random duration t' chosen from f_O. We then estimate P_S as the fraction of microdomains whose clusters reach $n \approx N x_b$ within that time. In Fig. 3 the predictions of Eq. (7) are compared with the numerical simulations. As shown, the agreement is quite good. In the following section we also compute the spark rates R_S numerically by counting the number of sparks recruited in 1 ms intervals.

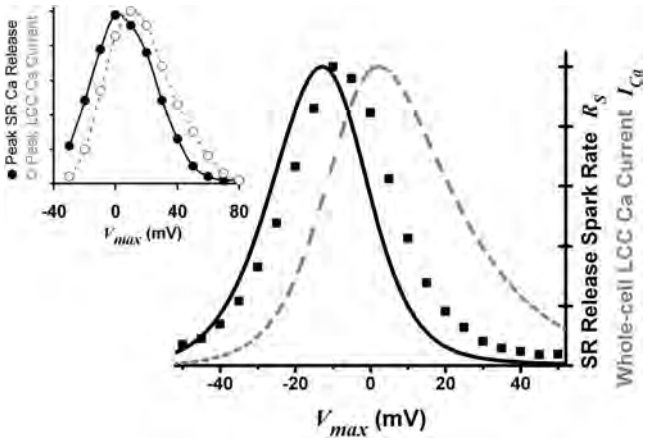

FIG. 4. Analytical (solid line) and numerically simulated (■) spark rate R_S as a function of V_{max} ($g=0.910$ $\mu m^3\,s^{-1}$); whole-cell I_{Ca} (dashed line). Inset: Experimental values from [4] for peak SR release current (•) and peak LCC current (◦). (All plots normalized to peak height.)

Graded release and comparison to experiments: In experiments, the relationship between Ca entry and Ca release can be assessed by depolarizing the membrane to various test voltages V_{max}. The peak total currents for LCC-mediated Ca entry and RyR-mediated Ca release from the SR are then measured following the depolarization. In Fig. 4 (inset) we reproduce the classic experimental data of Wier *et al.* [4]; it shows that *both* Ca release from the SR and Ca entry via the LCC have a bell-shaped functional dependence on V_{max}, but their relation with each other is nontrivial as evidenced by their relative shift. Since the amount of Ca released from the SR is determined by the spark recruitment rate, the behavior manifest in this data should be reflected in the spark rate R_S as a function of V_{max}.

Figure 4 shows the peak spark rates due to a depolarization to V_{max}, using our analytically calculated P_S from Eq. (7) in Eq. (1), as well as a simulation of $N_d=100{,}000$ independent microdomains with Markov-governed LCCs initialized in state C_2. Also plotted is the peak whole-cell Ca current entering the cell via LCCs estimated by $I_{Ca}=N_d P_o(V_{max}) i_{Ca}(V_{max})$, where $P_o(V_{max})$ is the steady-state open probability of the LCC. It is evident from Fig. 4 that our results reproduces semi-quantitatively the experimentally observed graded release behavior including the *correct relative shift* of the two relevant curves. As one would expect, the more exact numerical simulations are closer quantitatively to the experimental behavior, however the analytical results are remarkably close.

The graded relationship between whole-cell Ca release and Ca entry is reflected in the spark recruitment rate [Eq. (1)]. For large negative V_{max}, i_{Ca} is large and every LCC opening, although rare, will trigger a spark. In this regime the spark rate is dominated by the voltage dependence of the trigger mechanism via P_{C1} (which roughly follows P_o, since

α and β are fast voltage-independent rates.) As V_{max} is increased further and the single channel current i_{Ca} weakens, P_S is reduced and the probability of responding to the trigger is less; concurrently, I_{Ca} also decreases. The negative-voltage bias in Ca release reflects a preference for high Ca current strength (i_{Ca}) at negative voltages (where microdomain Ca entry is rare but strong) as opposed to high availability (P_o) at positive voltages (where microdomain Ca entry is frequent but weak). Hence, our model quantified by Eq. (1) explains experimentally measured whole-cell properties in terms of the kinetics of ion channels in Ca microdomains. A more detailed analysis of the analytic prediction will be presented in a future publication.

In this paper we have analyzed the stochastic properties of Ca signaling at both the whole-cell and ion channel level. The main result is an analytic description of the relationship between single channel kinetics and the aggregate whole-cell response. In the context of the cardiac cell, we have reproduced and analytically explained the important voltage-dependent relationships observed experimentally. This work should pave the way to a more detailed understanding of Ca signaling in a wide range of biological processes.

ACKNOWLEDGMENTS

This work is supported by the NSF and NIH/NHLBI P01 HL078931. R.R. thanks Tom Chou and Vladimir Minin for valuable discussions. Y.S. thanks A. Karma for valuable discussions, and the KITP Santa Barbara, where part of this work was completed.

[1] M. Falcke, Adv. Phys. **53**, 255 (2004).
[2] M. J. Berridge, Cell Calcium **40**, 405 (2006).
[3] D. M. Bers, *Excitation-Contraction Coupling and Cardiac Contractile Force (Developments in Cardiovascular Medicine)* (Springer, Berlin, 2006).
[4] W. G. Wier, T. M. Egan, J. R. Lopez-Lopez, and C. W. Balke, J. Physiol. (London) **474**, 463 (1994).
[5] M. D. Stern, Biophys. J. **63**, 497 (1992).
[6] J. L. Greenstein, R. Hinch, and R. L. Winslow, Biophys. J. **90**, 77 (2006).
[7] C. Soeller and M. B. Cannell, Prog. Biophys. Mol. Biol. **85**, 141 (2004).
[8] J. J. Rice, M. S. Jafri, and R. L. Winslow, Biophys. J. **77**, 1871 (1999).
[9] M. D. Stern, L. S. Song, H. Cheng, J. S. Sham, H. T. Yang, K. R. Boheler, and E. Rios, J. Gen. Physiol. **113**, 469 (1999).
[10] A. J. Tanskanen, J. L. Greenstein, A. Chen, S. X. Sun, and R. L. Winslow, Biophys. J. **92**, 3379 (2007).
[11] J.-W. Shuai and P. Jung, Biophys. J. **83**, 87 (2002).
[12] R. Hinch, Biophys. J. **86**, 1293 (2004).
[13] M. Bár, M. Falcke, H. Levine, and L. S. Tsimring, Phys. Rev. Lett. **84**, 5664 (2000).
[14] A. Cavalie, D. Pelzer, and W. Trautwein, Pfluegers Arch. **406**, 241 (1986).
[15] A. Zahradnikova, I. Zahradnik, I. Gyorke, and S. Gyorke, J. Gen. Physiol. **114**, 787 (1999).
[16] L. Cleemann, W. Wang, and M. Morad, Proc. Natl. Acad. Sci. U.S.A. **95**, 10984 (1998).
[17] Y. Shiferaw, M. A. Watanabe, A. Garfinkel, J. N. Weiss, and A. Karma, Biophys. J. **85**, 3666 (2003).
[18] G. Langer and A. Peskoff, Biophys. J. **70**, 1169 (1996).
[19] R. Thul and M. Falcke, Phys. Rev. E **73**, 061923 (2006).
[20] C. W. Gardiner, *Handbook of Stochastic Methods* (Springer-Verlag, Berlin, 1990).
[21] R. F. Fox and Y. N. Lu, Phys. Rev. E **49**, 3421 (1994).
[22] D. A. Darling and A. J. F. Siegert, Ann. Math. Stat. **24**, 624 (1953).
[23] M. Abramowitz and I. Stegun, *Handbook of Mathematical Functions with Formulas, Graphs, and Mathematical Tables* (Dover, New York, 1964).
[24] We approximate current through an open LCC with $i_{Ca}=P_{Ca}\phi(\beta_{Ca}C_{ext})/(e^{\phi}-1)$ fmol s^{-1} where $\phi=2VF/RT$ for voltage V (mV), with permeability $P_{Ca}=0.913$ μm^3 μs^{-1}, $\beta_{Ca}=0.341$, extracellular [Ca] $C_{ext}=2000$ μM, $F=96.5$ C mmol^{-1}, $R=8.314$ J M^{-1} K^{-1}, $T=310$ K. Rates for the LCC Markov scheme (Fig. 1) are $\alpha_1(V)=(1+e^{(V-2)/7})$ms^{-1}, $\beta_1(V)=2.35$ ms^{-1}, $\alpha=1/9$ ms^{-1} and $\beta=1$ ms^{-1}. Other physiological parameters are $\tau=4.4$ μs, $v=1.26\times10^{-3}$ μm^3, $c_{sr}=1000$ μM, $c_o=0.1$ μM, $k_+=0.0005$ μM^{-2} ms^{-1}, and $k_-=2$ ms^{-1}.